P1.9 Performance and Application of a Multi-wavelength, Ground-based Microwave Radiometer in Rain Nowcasting

P.W. Chan * and C.M. Tam
Hong Kong Observatory, Hong Kong, China

1. INTRODUCTION

In operational weather forecasting, it is a common practice to examine the temperature and humidity profiles measured by radiosondes and the derived instability indices in nowcasting heavy rain and thunderstorms. However, radiosonde measurements are available only twice a day and, during rain episodes, thermodynamic properties of the troposphere normally would change rapidly in between measurements, especially in subtropical coastal areas like Hong Kong. More frequently available thermodynamic information, together with wind data up to the upper troposphere (e.g. from radar wind profilers, Chan and Yeung (2003)), would greatly benefit severe weather nowcasting.

Ground-based microwave radiometers (Rose and Czekala 2003, Ware et al. 2004) retrieve the temperature and humidity profiles up to 10 km by measuring the radiation intensity at a number of channels in the microwave spectrum that are dominated by atmospheric water vapor, cloud liquid water and molecular oxygen emissions. These profiles are available nearly continuously, at around one minute intervals. They are mainly used in non-precipitating conditions because the radiometer measurements become less accurate in the presence of a water film on the outer housing (radome). Recently there are some progress in applying rain-effect mitigation methods to the radiometer, such as a hydrophobic radome and forced airflow over the radome surface. As a result, reasonably accurate thermodynamic profiles are obtained in a rainfall rate up to 15 mm/hour (Ware et al., 2004). However, this rainfall rate is still much lower than that observed in typical heavy rain episodes in the subtropical areas, which normally reaches at least 30 mm/hour.

This paper presents the performance and application of a multi-wavelength, ground-based microwave radiometer for the nowcasting of heavy rain and thunderstorms in a field experiment conducted in Hong Kong in 2004. The equipment setup of the experiment is described in Section 2. Accuracy of the temperature and humidity profiles as well as precipitable water vapour (PWV) from the radiometer is first studied by comparing with measurements from the radiosonde, a wind profiler/RASS and Global Positioning System (GPS) receivers in Sections 3 to 5. Performance of the radiometer data in a rain episode is described in Section 6, which suggests that there is a certain degree of correlation between the instability index of the troposphere as calculated from the radiometer data and the occurrence of lightning flashes. This relationship is studied further in Section 7. Conclusion of this paper is given in Section 8.

* *Corresponding author address:* P.W. Chan, Hong Kong Observatory, 134A Nathan Road, Hong Kong
email: pwchan@hko.gov.hk

2. EQUIPMENT SETUP

The radiometer in this study (same as that in Ware et al. 2004) measures the radiation intensity at 7 oxygen channels (51-59 GHz) and 5 water-vapour channels (22-30 GHz) to obtain the temperature and humidity profiles. It is equipped with a hydrophobic radome surface and a blower of heated air over the radome to minimize the effect of rain. During the field experiment, the radiometer was configured to make both zenith scans and elevation scans at a fixed angle. Following the general practice (e.g. Hewison et al. 2004 and Ware et al. 2004), only the zenith scan data are used in this paper to retrieve the thermodynamic profiles of the troposphere up to 10 km, which are normally available every 5 minutes.

Retrieval of temperature and humidity profiles from the radiation intensity measurements of the radiometer is accomplished by neural network methods based on historical radiosonde data, using a radiative transfer model to simulate the observations of a radiometer (Ware et al. 2004). In this study, the neural network was trained by a high-resolution radiosonde dataset with a data availability rate of 0.5 Hz during the ascent of the balloon (which translates to a spatial resolution of around 10 m for the typical ascent speed). Radiosonde data of a whole year (2003) were used.

The field experiment was conducted in Hong Kong from February to June 2004. The radiometer was placed at three locations and its data are compared with those from the radiosonde, a wind profiler/RASS and GPS receivers (Figure 1). In studying the thermodynamic index given by the radiometer, we also refer to the data from a lightning location network (Murphy and Cummins 2000), which detects cloud-to-ground flashes up to about 100 km from Hong Kong.

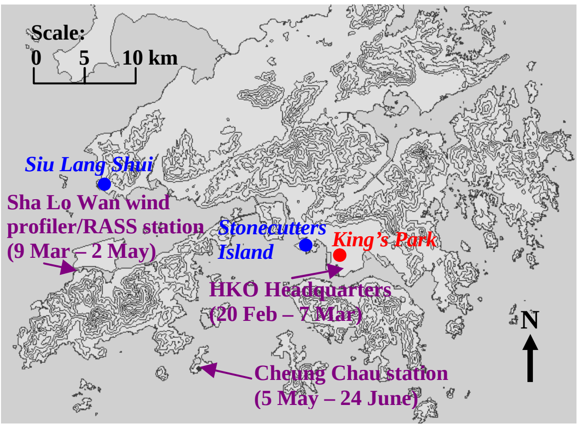

Figure 1 Map of Hong Kong (height contours: 100 m). The radiometer was set up at three locations (names in purple) for the periods indicated in parenthesis. The radiosonde station (red) and the two GPS receivers mentioned in this paper (blue) are also shown. HKO refers to Hong Kong Observatory.

3. COMPARISON WITH RADIOSONDE

Temperature and humidity profiles from the radiometer are compared with those from the radiosonde launched at King's Park. Their biases and standard deviations with respect to the radiosonde measurements are shown in Figure 2. The followings are observed about the radiometer:-

(a) For temperature, there is a warm bias up to about 1.4 km and a cold bias further aloft. The standard deviation increases gradually with height, but is generally smaller than about 2 degrees Celsius.

(b) For relative humidity, there is a wet bias between about 1.2 km and 5.8 km, and a dry bias higher up. The standard deviation again increases with height, but is mainly below 20%.

The above results are generally consistent with those obtained in other studies of the same kind of ground-based radiometer (e.g. Hewison et al. 2004, which studies radiometer data up to 4 km).

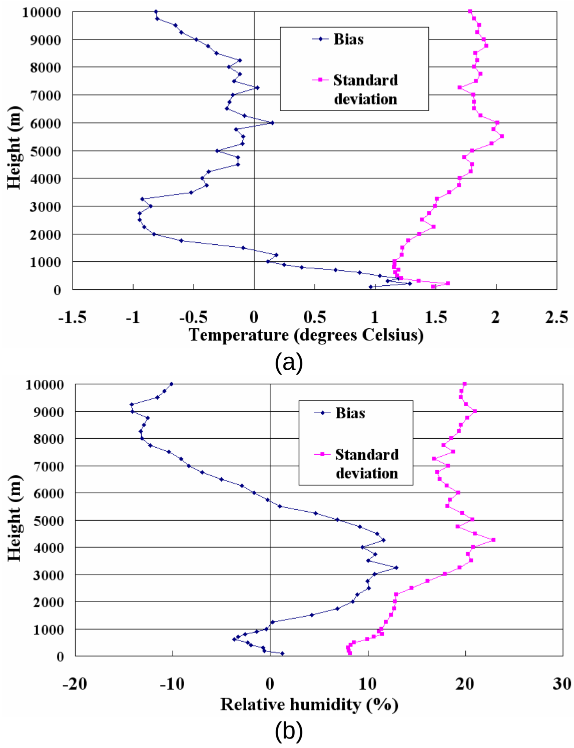

Figure 2 The biases and standard deviations of the radiometer measurements with respect to the concurrent radiosonde data.

Since the relative humidity data have a greater impact on the application of the radiometer to rain nowcasting, we select to study the humidity profiles from the radiometer in more detail. First of all, the wet bias of the radiometer in the mid-troposphere is related to the occasional occurrence of an elevated, moist layer that is not measured by the radiosonde (an example in Figure 3). This moist layer appeared more frequently in the latter part of the field experiment, sometimes close to saturation. It points to a need to review the radiative transfer model employed by the radiometer for the summer monsoonal weather in southern China, but this is outside the scope of the present paper. Secondly, about the dry bias in the upper troposphere (Figure 3), it seems that the radiometer basically relies on the climatological profile at those altitudes, which is a general decrease of the relative humidity with height. But sometimes the upper troposphere becomes more humid than normal in the summer-time due to the presence of high cirrus clouds (e.g. from the upper-level outflow of a rainband). Retrieval of the humidity profile at these heights may be improved by incorporating the brightness temperature measurements from geostationary meteorological satellites (Liljegren, 2004).

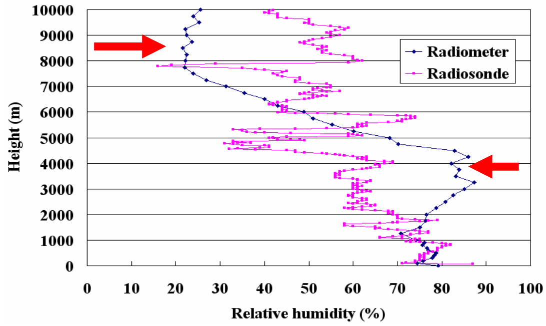

Figure 3 The relative humidity profiles from the radiometer and the radiosonde at 00 UTC, 31 May 2004, showing the wet bias in the middle troposphere and dry bias in the upper troposphere (red arrows).

For nowcasting of rain, K-index (KI) is calculated from the temperature and humidity profiles of the radiometer,

$$KI = (T_{850} - T_{500}) + Td_{850} - (T_{700} - Td_{700})$$

where T is the temperature, Td is the dew point and subscripts are the pressure levels (in hPa). Radiometer data are given in heights, and the corresponding pressure levels are determined by assuming hydrostatic approximation. K-indices from the radiometer and the radiosonde are compared in Figure 4. They are found to correlate well, with a correlation coefficient of 0.856. The radiometer tends to give a slightly larger K-index because there is occasionally an elevated, moist layer (as discussed above) and the dew-point depression in the middle troposphere (700 hPa, which is about 3 km for southern China) is included in the K-index. Nonetheless, in view of all the above comparison results with the radiosonde, the radiometer is considered to provide reasonably accurate temperature and humidity profiles for rain nowcasting.

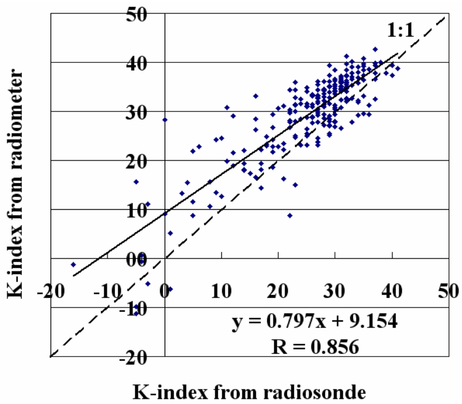

Figure 4 Comparison of the K-index from the radiosonde and the radiometer.

4. COMPARISON WITH WIND PROFILER/RASS

During installation at Sha Lo Wan (Figure 1), the radiometer measurements are also used to calculate virtual temperatures for comparison with those from a co-located wind profiler/RASS, which is a 1299-MHz system similar to the one discussed in Chan and Yeung (2003). The comparison results are shown in Figure 5. Once again, there is a warm bias of 0.5 – 1 degree Celsius within the boundary layer, and the standard deviation ranges between 1 and 1.5 degrees. All these are basically same as the comparison results with the radiosonde (Figure 2a). So it appears that the slight warm bias of the radiometer measurement in the boundary layer is not much related to the location difference of the radiometer and the reference instrument (radiosonde or wind profiler/RASS), and could be an inherent property of the radiometer itself.

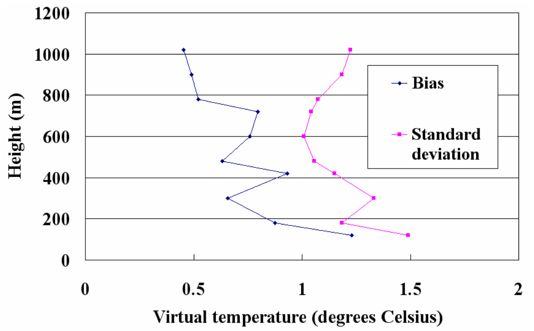

Figure 5 The bias and standard deviation of the virtual temperature from the radiometer with respect to the concurrent data from a wind profiler/RASS.

5. COMPARISON WITH GPS RECEIVERS

The precipitable water vapour (PWV) data from the GPS receiver closest to the location of the radiometer are used in the comparison, namely, the GPS receiver at Stonecutters Island when the radiometer was placed at Hong Kong Observatory headquarters and Cheung Chau, and the one at Siu Lang Shui when the radiometer was moved to Sha Lo Wan (locations all shown in Figure 1). The comparison results are shown in Figure 6. The two measurements are correlated well, with a correlation coefficient exceeding 0.9.

Relatively large discrepancies are occasionally observed between the two measurements. For instance, for the data-points encircled in Figure 6, the PWV from the radiometer is larger than that from the nearest GPS receiver by 10 mm or more. An example of such a case is shown in Figure 7. The radiometer was placed at Cheung Chau at that time, and it was co-located with a tipping-bucket rain gauge with a resolution of 0.5 mm. It appears from this case that, when the rain is heavy (at a maximum rate of 0.5 mm/min. = 30 mm/hour, as also indicated in the rainfall estimation from the weather radar [not shown]) but not continuous, the PWV values from the radiometer and the GPS receivers are generally consistent with each other (e.g. before 6 a.m. and after 7 a.m. in Hong Kong time, which is 8 hours ahead of UTC). But when the rain is heavy and more or less continuous (between 6 and 7 a.m.), the PWV from the radiometer exhibits rather rapid fluctuations that are not observed in the GPS data. The two measurements could differ by more than 10 mm at times (e.g. at 6:31 a.m., indicated by a red arrow). To ascertain that this difference is not due to local variation of rainfall rate, we have consulted the rainfall measurements from a network of rain gauges in Hong Kong and the weather radar imageries. The rainfall rates are found to be about the same at the locations of the radiometer and the two GPS receivers (not shown). The radiometer data at these moments are considered to be doubtful and they will not be used, for instance, to calculate the temporally averaged K-index in Section 7.

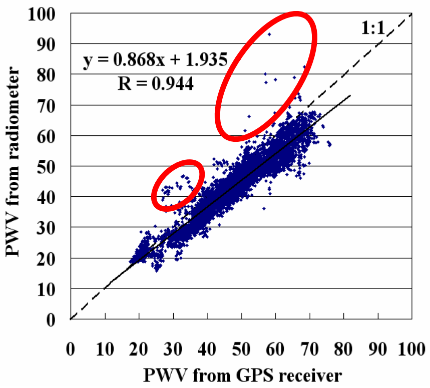

Figure 6 Comparison of PWV from the GPS receivers and the radiometer. The two measurements sometimes differ by 10 mm or more (e.g. data points enclosed in red).

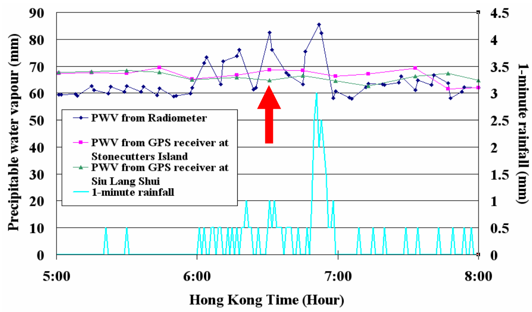

Figure 7 PWV from the radiometer and the GPS receivers as well as the 1-minute rainfall measured at the radiometer's location (Cheung Chau) in the morning of 8 May 2004. A doubtful piece of data from the radiometer is indicated by a red arrow.

6. A CASE STUDY

The heavy rain episode in the afternoon of 17 April 2004 is highlighted here as an example of the application of the radiometer in rain nowcasting. Synoptically, a trough of low pressure lingered near the south China coast on that day (Figure 8). Weather radar imageries (an example in Figure 9)

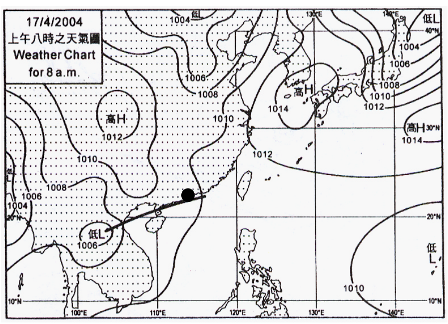

Figure 8 Surface isobaric chart at 8 a.m., 17 April 2004.

show that a rainband tracked basically eastwards across Hong Kong between 3:30 p.m. and 8 p.m., bringing more than 60 mm of rain to many parts of the territory. Lightning flashes inside Hong Kong are found to be mainly associated with the radar echoes with a reflectivity of at least 44 dBz at 3 km AMSL (equivalent to a rainfall rate of about 20 mm/hour). The part of the radar echoes reaching this reflectivity has a typical width (along the direction of movement of the rain band) of around 20 km (Figure 9).

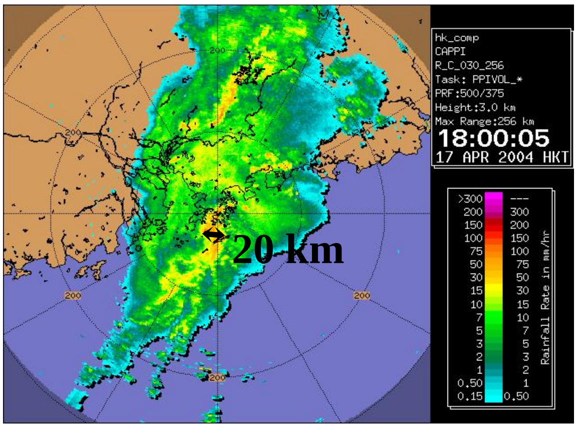

Figure 9 Weather radar imagery at 3 km AMSL at 6 p.m., 17 April 2004.

The radiometer shows that, with the approach of the rainband to Hong Kong, relative humidity increased gradually at all altitudes (Figure 10). It reached a maximum at around 2 km, where synoptically a fresh to strong southwesterly airstream brought relatively moist air from the South China Sea to the coast of southern China. The radiometer also gives a gradual decrease of the cloud-base height, which is consistent with human weather observations. During the period of heavy rain, the air was near saturation below 3 km or so, and the liquid water content had a maximum value of about 4.9 g/m^3. As the rainband moved away from Hong Kong, relative humidity decreased and the cloud base lifted gradually.

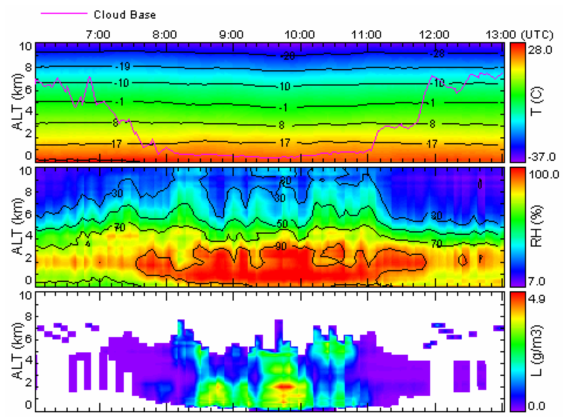

Figure 10 The time-height plots of the radiometer data between 2 p.m. (06 UTC) and 9 p.m. (13 UTC) of 17 April 2004. The upper panel shows the temperature and the cloud-base height. The middle panel is the relative humidity. The lower one is the liquid water content. (The plots are generated by the software "Vizmet" bundled with the radiometer.)

The accumulation of water vapour at about 2 km and the gradual rise of relative humidity at all altitudes as measured by the radiometer are good indications of the imminence of heavy rain. Alternatively, they can be expressed in terms of the K-index calculated from the radiometer data (Figure 11). With the approach of the rainband to Hong Kong, K-index rose steadily. It exceeded 35 when heavy rain started to take place and the lightning flashes became active. After about 6:30 p.m., K-index began to fall, rain eased off gradually and there were no more lightning activities in the vicinity of the radiometer.

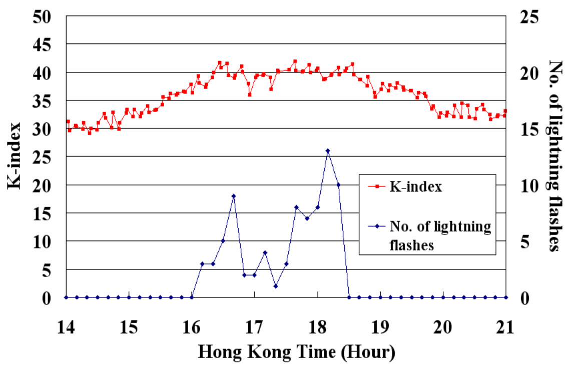

Figure 11 K-index calculated from the radiometer data and the number of lightning flashes within 20 km from the radiometer in the afternoon of 17 April 2004.

7. CORRELATION BETWEEN K-INDEX AND LIGHTNING FLASHES

K-index is a commonly used tool for assessing the chance of thunderstorms. Since radiosondes are normally available twice a day, the K-index calculated from radiosonde measurements can only be used in the assessment for the next 12 hours or so, in the form of rules of thumb or flow charts in combination with other meteorological factors (e.g. Collier and Lilley (1994)). Radiometer provides frequently updated temperature and humidity profiles of the troposphere for calculating K-index and offers a unique opportunity for a more quantitative study of the correlation between K-index and the degree of tropospheric instability, which is related to the occurrence of thunderstorms.

During the field experiment, it was observed in many rain episodes that lightning flashes in the vicinity of the radiometer became more frequent when the K-index calculated from the radiometer data exceeded about 35 (as in the case of 17 April 2004, Figure 11). For each rain episode, a temporally averaged K-index for the period when K-index reaches 35 or above is calculated. Tropospheric instability is expressed in terms of the lightning flashes in the following ways:-

(a) the total number of lightning flashes within a certain range *R* from the radiometer during the period when the K-index calculated from the radiometer is at least 35;

(b) the frequency of lightning flashes, which equals the total number of lightning flashes defined in (a) above divided by the period (in hours) when the K-index from the radiometer is at least 35.

The range *R* from the radiometer is varied between10 km and 100 km for a statistical study of the correlation between the temporally averaged K-index from the radiometer and the tropospheric instability as defined in (a) and (b) above. The latter *R* limit is based on the maximum detection range of the lightning location network. The former one is chosen so that there is a reasonably large sample of cases (at least 10) for a statistical study. As *R* is reduced further, the number of rain episodes with lightning activity within *R* from the radiometer decreases dramatically.

This paper focuses on the lightning activity associated with rainbands in the summer monsoon over southern China. There are altogether 11 cases. Rain episodes involving isolated thunderstorms (for instance, triggered by prolonged periods of solar heating over inland areas of southern China) are not considered.

It is found that the correlation reaches a maximum at both *R* = 10 km and 20 km for lightning flash number, whereas it is the largest at *R* = 20 km for lightning flash frequency (Figure 12). The *R* value of 20 km is consistent with the radar observations of the spatial scale of the rainbands with active lightning (e.g. Figure 9). For both lightning flash number and frequency, the correlation with the temporally averaged K-index decreases as *R* exceeds 20 km. It starts to level at *R* = 60 km, as the lightning flash dataset for each rain episode is more or less exhausted.

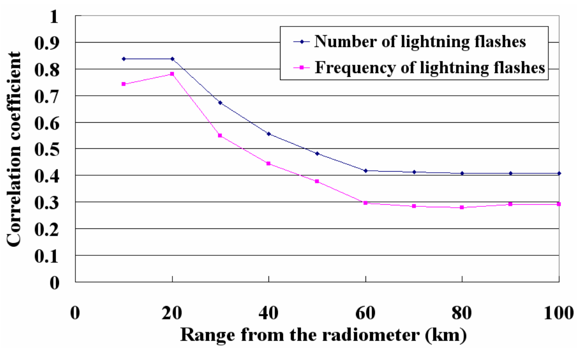

Figure 12 Correlation coefficient between the temporally averaged K-index and the lightning activity (total number or frequency of lightning flashes) as a function of the range from the radiometer.

The scatter plots of the temporally averaged K-index against the lightning flash number and frequency within 20 km from the radiometer are shown in Figure 13. The correlation is relatively high, with a correlation coefficient of about 0.8. For the lightning flash number, the slope of the least-square linear fit is 1.183. That means, when the temporally averaged K-index is increased by 1, the number of lightning flashes within 20 km from the radiometer will on average increase by a factor of $10^{1/1.183} = 7$. Similarly, for the frequency of lightning flashes, the corresponding increase will be a factor of $10^{1/1.276} = 6$. Thus, the lightning activity is rather sensitive to the value of K-index.

As shown in Figure 13, the heavy rain episode on 8 May has the largest values of temporally averaged K-index and the total number of lightning flashes as well as the second highest frequency of lightning flashes among all the rain episodes

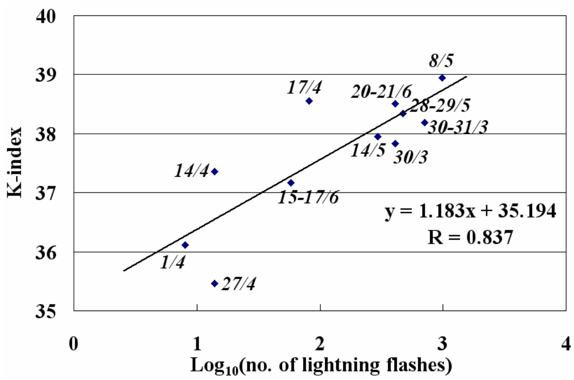

(a)

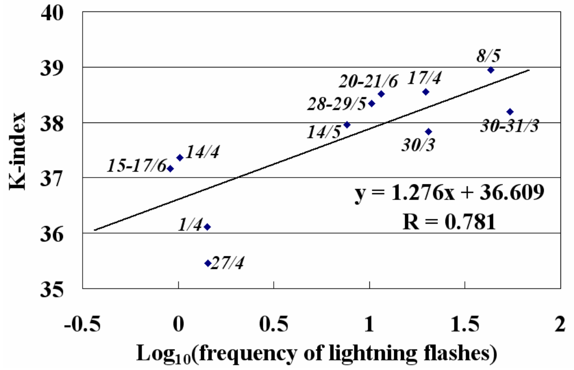

(b)

Figure 13 Scatter plots of the temporally averaged K-index against the number (a) and the frequency (b) of lightning flashes within 20 km from the radiometer. Dates of the rain episodes are marked nearby the data point (in the form of day/month).

considered. It is in fact the only episode in the rain season of Hong Kong in 2004 that necessitated the issuance of "black rainstorm warning" by the Hong Kong Observatory, which means very heavy rain has fallen generally over Hong Kong, exceeding 70 mm in an hour. A meso-cyclone was observed to pass over the radiometer's location (Cheung Chau), as analyzed in Li et al. 2004.

It should be noted that the above analysis is based on a rather limited dataset (a total of 11 rain episodes) in the summer monsoonal season of a year only (2004). The robustness of the results is yet to be studied with a larger dataset.

8. CONCLUSION

Performance and application of a multi-channel, ground-based microwave radiometer in rain nowcasting is studied in this paper. The radiometer was equipped with a hydrophobic radome surface and a blower of heated air to mitigate the adverse effect of a rain-coated radome on the measurement accuracy. It was found to give reasonably accurate temperature and humidity profiles as well as precipitable water vapour (PWV) with reference to the measurements from the radiosonde, a wind profiler/RASS and GPS receivers. However, some discrepancies between the data from the radiometer and the reference instruments were observed:-

(a) Temperatures from the radiometer showed a warm bias within the boundary layer.
(b) Relative humidity profile from the radiometer

tended to show an elevated, moist layer at 3 to 4 km. This resulted in a generally larger K-index as compared with the value calculated from the radiosonde measurement.

(c) Under continuous rain with a rate of 30 mm/hour or more, PWV from the radiometer exhibited rapid fluctuations that were not observed in GPS measurements, and the radiometer data appeared to be doubtful.

Despite these discrepancies, the radiometer was found to provide useful information for rain nowcasting, e.g. increase of relative humidity at all altitudes, and the accumulation of water vapour in the lower troposphere. K-index was also calculated from the frequently updated temperature and humidity profiles from the radiometer for nowcasting purpose. Heavy rain with active lightning mostly occurred when K-index stayed above 35 or so.

A temporally averaged K-index for the period when K-index was 35 or above was determined from the radiometer data. For the summer monsoonal rain in southern China, it was found to correlate well with the total number and the frequency of lightning flashes within 20 km from the radiometer (which was consistent with the radar observations of the spatial scale of the rainbands with active lightning). The lightning activity turned out to be rather sensitive to the K-index value: when K-index rose by 1, the number and the frequency of lightning flashes would increase by a factor of 7 and 6 respectively. Continuous availability of the temperature and humidity profiles of the troposphere from the radiometer enabled a quantitative study of the correlation between K-index and the atmospheric instability (expressed in terms of the lightning activity), which could not be achieved by using the twice-daily radiosonde measurements alone.

Acknowledgement

The authors would like to thank the Lands Department of the Government of the Hong Kong Special Administrative Region for providing the GPS receiver data in this study. The PWV data derived from GPS receivers are produced in a joint research project between the Hong Kong Observatory and the Hong Kong Polytechnic University. Thanks also go to China Light and Power Limited, which provides the lightning flash data from the lightning location network in Hong Kong.

References

Chan, P.W., and K.K. Yeung, 2003: Experimental extension of the measurement range of a boundary layer wind profiler to about 9 km. *Preprints, 12th Symposium on Meteorological Observation and Instrumentation,* Amer. Meteor. Soc.

Collier, C. G., and R. B. E. Lilley, 1994: Forecasting thunderstorm initiation in north-west Europe using thermodynamic indices, satellite and radar data. *Meteor. Appl.*, **1**, p.75-84.

Hewison, T., and coauthors, 2004: Monitoring inversions from ground-based remote sensing instruments during Temperature, Humidity, and Cloud profiling campaign (TUC). *Preprints, 8th Specialist Meeting on Microwave Radiometry and Remote Sensing Applications.*

Li, L.O., C.C. Lam and W.K. Wong, 2004: The meso-cyclone over Hong Kong on 8 May 2004: Doppler radar observation and numerical simulation. *Preprints, International Conference on Mesoscale Convective Systems and Heavy Rainfall in East Asia (ICMCS-IV)*, Chinese Academy of Meteorological Sciences and China Meteorological Administration.

Liljegren, J., 2004: Improved retrievals of temperature and water vapor profiles with a twelve-channel radiometer. *Preprints, 8th Symposium on Integrated Observing and Assimilation Systems for Atmosphere, Oceans, and Land Surface (IOAS-AOLS)*, Amer. Meteor. Soc.

Murphy, M.J., and K.L. Cummins, 2000: Early detection and warning of cloud-to-ground lightning at a point of interest. *Preprints, 2nd Symposium on Environmental Applications,* Amer. Meteor. Soc.

Rose, T., and H. Czekala, 2003: Filter bank radiometers for atmospheric profiling. *Preprints, Sixth International Symposium on Tropospheric Profiling: Needs and Technologies,* p.261-263.

Ware, R., P. Herzegh, F. Vandenberghe, J. Vivekanandan, and E. Westwater, 2004: Ground-based radiometeric profiling during dynamic weather conditions. *Submitted to J. Appl. Meteor.*